

A Donor–Acceptor 10-Cycloparaphenylene and Its Use as an Emitter in an Organic Light-Emitting Diode

Dongyang Chen, Yoshimasa Wada, Yu Kusakabe, Liansheng Sun, Eiichi Kayahara, Katsuaki Suzuki, Hiroyuki Tanaka, Shigeru Yamago,* Hironori Kaji,* and Eli Zysman-Colman*



Cite This: <https://doi.org/10.1021/acs.orglett.3c00127>



Read Online

ACCESS |



Metrics & More



Article Recommendations



Supporting Information

ABSTRACT: Here, we explored the possibility of using cycloparaphenylenes (CPP) within a donor–acceptor TADF emitter design. 4PXZPh-[10]CPP contains four electron-donating moieties connected to a [10]CPP. In the 15 wt % doped in CzSi film, 4PXZPh-[10]CPP showed sky-blue emission with $\lambda_{\text{PL}} = 475$ nm, $\Phi_{\text{PL}} = 29\%$, and triexponential emission decays with τ_{PL} of 4.4, 46.3, and 907.8 ns. Solution-processed OLEDs using 4PXZPh-[10]CPP exhibited sky-blue emission with an λ_{EL} of 465 nm and an EQE_{max} of 1.0%.



Cycloparaphenylenes (CPPs) are the smallest building blocks of “armchair” carbon nanotubes and have attracted increasing attention due to their naturally curved nanostructure, which makes them well suited as templates for host–guest chemistry and the bottom-up synthesis of carbon nanotubes.^{2–4} Moreover, their curved and radially oriented π -system has generated increasing interest from the organic semiconductor community.^{5–7} The aesthetically beautiful structure belies the significant embedded strain that results from the distorted benzene rings in the nanostructure, particularly the smaller analogues, which renders their synthesis challenging. The first CPPs ([9]CPP, [12]CPP, and [18]CPP) were synthesized using a strategy where cyclohexadienes were employed to afford intermediates that could more easily accommodate the curved structure prior to aromatization in the final step.⁸ A complementary strategy involves the formation of platinum complexes as precursors that then can be demetalated to form the CPP by reductive elimination. Seminal contributions from Bertozzi and Jasti et al.,⁸ Itami et al.,⁹ and Yamago et al.,¹⁰ among others, have demonstrated how the synthesis of CPPs can be scaled and how these structures can be elaborated further to generate compounds with desirable optoelectronic properties.^{11–17}

The optoelectronic properties of CPPs can be tuned by decoration with electron-donating or -withdrawing groups.¹⁸ Jasti et al. incorporated the electron acceptor benzothiadiazole (BT) into the ring to construct donor–acceptor macrocycles BT[10]CPP (Figure 1).¹⁹ The DFT calculations revealed that the LUMO of BT[10]CPP is localized on the acceptor moiety and the LUMO level is stabilized by 0.8 eV compared to the reference [10]CPP, while the HOMOs are located on the remaining benzene rings on the macrocycle and are slightly destabilized compared to that of [10]CPP.¹⁹ The donor–

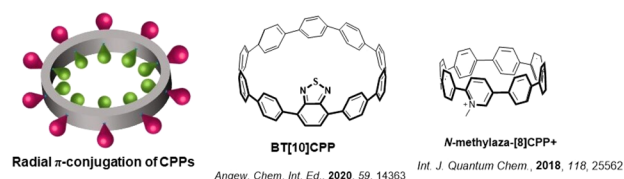


Figure 1. Molecular structures of cycloparaphenylene based D–A emitters. Middle and right images reprinted with permission from refs 19 and 20. Copyrights 2020 and 2017 Wiley.

acceptor (D–A) character of BT[10]CPP is evident in the absorption spectrum where a new band was observed at 450 nm, which correlates to the HOMO \rightarrow LUMO transition that is of charge transfer (CT) character as assigned by time-dependent DFT (TD-DFT) calculations. The emission spectrum of BT[10]CPP is red-shifted by more than 100 nm (3946 cm^{-1}) with a maximum emission wavelength (λ_{PL}) of 571 nm and a photoluminescence quantum yield (Φ_{PL}) of 59% in dichloromethane (DCM), compared to λ_{PL} of 466 nm and Φ_{PL} of 65% for [10]CPP; moreover, the emission spectrum red-shifts with increasing solvent polarity, which is consistent with emission from a state of CT character.¹⁹ Computational studies from Sancho-García et al. provided insight that incorporation of an electron-withdrawing group not only can affect the HOMO/LUMO distribution and

Received: January 12, 2023

energies but also can tune the singlet–triplet energy gap (ΔE_{ST}).²⁰ For the proposed molecule *N*-methylaza-[8]CPP⁺, where a methylpyridinium unit is incorporated into the CPP skeleton and used as an electron acceptor, the DFT calculations showed that the LUMO of *N*-methylaza-[8]CPP⁺ is located on the methylpyridinium unit as well as the adjacent benzene rings and the HOMO is located across the remaining benzene rings. As a result, the ΔE_{ST} was predicted to decrease from 0.50 eV for [8]CPP to 0.23 eV for *N*-methylaza-[8]CPP⁺.²⁰ This is the first evidence for the potential of this class of compounds to exhibit thermally activated delayed fluorescence (TADF), where a small ΔE_{ST} is required to promote reverse intersystem crossing (RISC) at ambient temperatures.²⁰

TADF compounds have generated much interest as these can be used as emitters in electroluminescent devices that are capable of harvesting both singlet and triplet excitons and their conversion to light.^{21–23} When the RISC occurs from the lowest excited triplet (T_1) to the lowest excited singlet (S_1) states, the RISC rate constant (k_{RISC}) is proportional to $|V_{SOC}|^2 \times \exp[-(\Delta E_{ST})^2]$, where $|V_{SOC}|^2$ is the spin–orbit coupling matrix element between T_1 and S_1 states and ΔE_{ST} is the energy gap between them.²⁴ A common strategy to enhance k_{RISC} and promote TADF is to minimize the ΔE_{ST} , which can be achieved by reducing the overlap integral between the HOMO and LUMO.^{25–27} Previous work on CPPs has demonstrated that CPP derivatives can exhibit CT character in their excited states and moderate HOMO/LUMO separation by suitable decoration of the CPP core; however, none of these CPP derivatives have been reported to show TADF. To act as potential high-performance emitters for OLEDs, it would be of strong interest to develop TADF CPP derivatives.^{20,28} In this work, we employed DFT and TD-DFT calculations using the Tamm–Dancoff approximation (TDA-DFT) to design the CPP-based TADF emitter 4PXZPh-[10]CPP, where four electron-donating moieties of 10-phenyl-10*H*-phenoxazine are connected to [10]CPP. The gas-phase calculations predict a ΔE_{ST} of 0.08 eV. Experimentally, 4PXZPh-[10]CPP shows weak CT emission in polar solvents. The Φ_{PL} is 29% in the 15 wt % doped thin film in 9-(4-*tert*-butylphenyl)-3,6-bis(triphenylsilyl)-9*H*-carbazole (CzSi). We demonstrate the first CPP-based solution-processed organic light-emitting diode (OLED), which shows sky-blue emission with a maximum external quantum efficiency, EQE_{max}, of 1.0%.

The synthesis of 4PXZPh-[10]CPP started from the tetra-trifluoromethanesulfonate-substituted [10]CPP (4OTf-[10]CPP), which was synthesized from the 2,5-di(3-butenyloxy)-1,4-benzquinone in 10 steps as previously reported.²⁹ 4OTf-[10]CPP reacted with the electron-donor moiety BpinPhPXZ under Suzuki–Miyaura cross-coupling conditions to obtain 4PXZPh-[10]CPP with a yield of 45% (Scheme 1).

To gain insight into the electronic structure of 4PXZPh-[10]CPP, DFT and TDA-DFT calculations were performed on both 4PXZPh-[10]CPP and the reference compound [10]CPP. The ground state (S_0), S_1 , T_1 , and higher triplet excited state (up to T_5) energies were calculated in the gas phase at the PBE0/6-31g(d,p) level of theory.^{30,31} As shown in Figure 2a, the HOMO and the pseudodegenerate HOMO–1 of 4PXZPh-[10]CPP are localized on two of the phenoxazine donors, respectively. The LUMO of 4PXZPh-[10]CPP is delocalized across the CPP acceptor moiety. For parent [10]CPP, the HOMO and LUMO are distributed across the

Scheme 1. Synthesis of 4PXZPh-[10]CPP

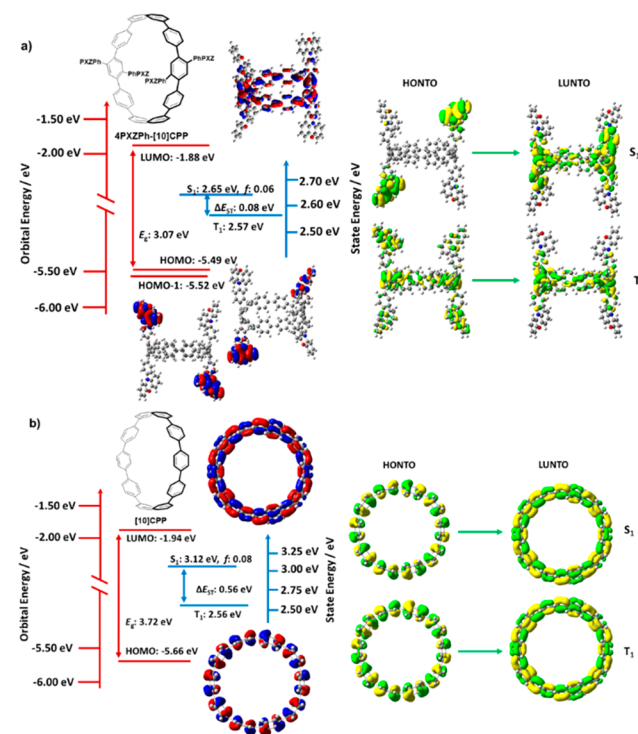
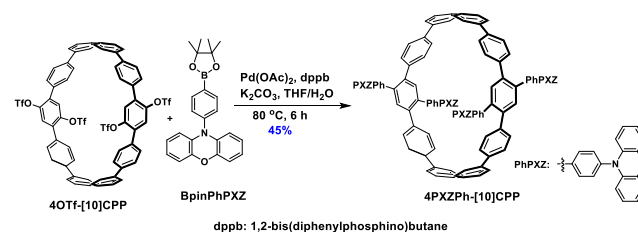


Figure 2. Theoretical modeling of the energies of the HOMO/LUMO and the S_1 and T_1 states of (a) 4PXZPh-[10]CPP and (b) reference compound [10]CPP in the gas phase and the electron density distribution of the frontier molecular orbitals (isovalue = 0.02).

whole molecule (Figure 2b). The HOMO of 4PXZPh-[10]CPP is destabilized to -5.49 eV compared to -5.66 eV for [10]CPP, while the LUMO of 4PXZPh-[10]CPP is slightly destabilized to -1.88 eV compared to -1.94 eV for [10]CPP, reflecting the small electronic communication between the donor moieties and the CPP skeleton. The spatially separated HOMO and LUMO ensures 4PXZPh-[10]CPP possesses a small ΔE_{ST} . TDA-DFT calculations indicate that the S_1 energy of 4PXZPh-[10]CPP (2.65 eV) is stabilized by 0.47 eV compared to that [10]CPP while the T_1 energy (2.57 eV) is slightly destabilized by 0.01 eV compared to [10]CPP, thereby resulting in a ΔE_{ST} of 0.08 eV for 4PXZPh-[10]CPP. The natural transition orbital (NTO) analysis of 4PXZPh-[10]CPP reveals a CT transition for S_1 from the PXZ donors to the CPP moiety, while the highest occupied NTO for T_1 is delocalized over the whole molecule and the lowest unoccupied NTO is located on the CPP moiety, which suggest a hybridized local and charge-transfer (HLCT) excited state (Figure S7).

Cyclic voltammetry (CV) and differential pulse voltammetry (DPV) were measured in dichloromethane (DCM) with *n*-

Bu_4NPF_6 as the supporting electrolyte to experimentally ascertain the HOMO and LUMO energy levels. The electrochemical behavior is detailed in the Supporting Information.

The photophysical properties of 4PXZPh-[10]CPP were investigated in both solution and films. Room-temperature ultraviolet–visible (UV–vis) absorption and PL spectra of 4PXZPh-[10]CPP and [10]CPP in dilute toluene solution are shown in Figure 3a. The absorption profile of 4PXZPh-

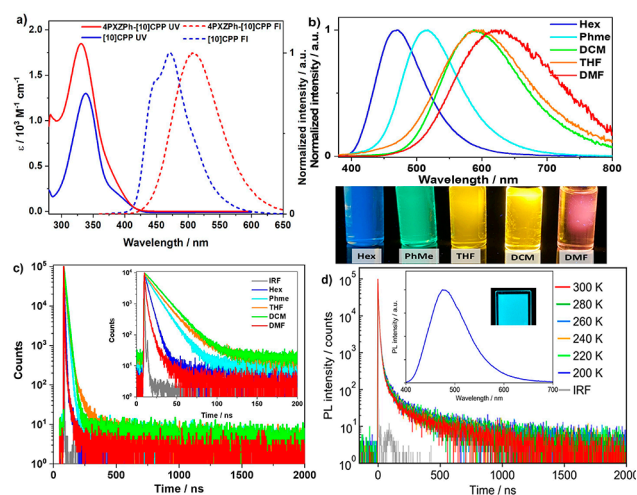


Figure 3. (a) Absorption and normalized emission spectra of 4PXZPh-[10]CPP and [10]CPP in toluene solution (10^{-5} M), the excitation wavelength, $\lambda_{\text{exc}} = 340$ nm, (b) solvatochromic emission study of 4PXZPh-[10]CPP ($\lambda_{\text{exc}} = 375$ nm), (c) transient PL decays of 4PXZPh-[10]CPP in different solvents ($\lambda_{\text{exc}} = 375$ nm), and (d) emission spectra (insert) and temperature-dependent transient PL decay spectra of 4PXZPh-[10]CPP/CzSi film ($\lambda_{\text{exc}} = 340$ nm).

[10]CPP is similar to that of [10]CPP with a slightly stronger absorption ($\epsilon = 1.0 \times 10^2 \text{ M}^{-1} \text{ cm}^{-1}$) at 400 nm, which is ascribed to a mixed LE and weak intramolecular CT (ICT) transition from HOMO to LUMO according to the TDA-DFT calculations. [10]CPP exhibits strong absorption at 340 nm, which is ascribed to a LE transition distributed across the CPP skeleton, while for 4PXZPh-[10]CPP the extra LE transition on the phenyl phenoxazine donor moieties are responsible for the moderately stronger and slightly blue-shifted absorption at 340 nm. The PL spectrum of 4PXZPh-[10]CPP is broad, unstructured, and red-shifted at $\lambda_{\text{PL}} = 508$ nm with Φ_{PL} of 34% compared to the vibrationally structured spectrum of [10]CPP at $\lambda_{\text{PL}} = 470$ nm with Φ_{PL} of 77%. The profiles of the two PL spectra suggest that the emissive state of 4PXZPh-[10]CPP is CT in nature while that of [10]CPP is LE in nature. The emission spectrum of 4PXZPh-[10]CPP is bathochromically shifted and becomes broader with increasing solvent polarity, behavior that is consistent with an emissive state of CT character (Figures 3b).

The time-resolved PL decays of 4PXZPh-[10]CPP were measured in solvents of different polarity. In nonpolar solvents of hexane (HEX), 4PXZPh-[10]CPP exhibits a prompt lifetime (τ_p) of 4.4 ns, while in more polar solvents such as toluene (PhMe), DCM, and tetrahydrofuran (THF), the τ_p values increase to 11.0, 14.5, and 13.6 ns, respectively. In the polar solvent dimethylformamide (DMF), the τ_p reduces to 3.1 ns. However, no delayed emission is observed in any of the solvents within a time window of 2 μs . The S_1 and T_1 energies

of 4PXZPh-[10]CPP were determined in both PhMe and DCM in 77 K. As shown in Figure S11, derived from the onset of the prompt fluorescence, the S_1 of 4PXZPh-[10]CPP in DCM is stabilized to 2.75 eV compared to 2.93 eV in PhMe, which led to a smaller ΔE_{ST} of 0.50 eV in DCM than 0.68 eV in PhMe as the T_1 is 2.25 eV in both solvents. However, compared to the TDA-DFT predicted excited-state energies (S_1 , 2.65 eV; T_1 , 2.57 eV), the T_1 measured in both toluene and DCM are strongly stabilized while the S_1 measured in toluene and DCM are stabilized by 0.28 and 0.10 eV, respectively, and this leads to a much larger experimentally determined ΔE_{ST} , which prohibits RISC from readily occurring at room temperature.

We next investigated the photophysics of 4PXZPh-[10]CPP in doped films. The host 9-(4-*tert*-butyl)phenyl)-3,6-bis-(triphenylsilyl)-9H-carbazole (CzSi) was chosen due to its suitable HOMO/LUMO levels and high triplet state energies. In the 15 wt % doped CzSi film, 4PXZPh-[10]CPP shows blue emission with $\lambda_{\text{PL}} = 475$ nm, $\Phi_{\text{PL}} = 29\%$, and $\tau_1 = 4.4$ ns, $\tau_2 = 46.3$ ns, and $\tau_3 = 907.8$ ns (Figure 3d). The temperature dependence of the transient PL decay in CzSi film was performed from 300 to 200 K. However, the delayed emission component in these films exhibited an increase with decreasing temperature, which implies that the emission is not TADF.^{32–34}

With a view to exploring the potential of 4PXZPh-[10]CPP as an emitter in OLEDs, a solution-processed OLED was fabricated using the architecture (Figure 4a) indium tin oxide

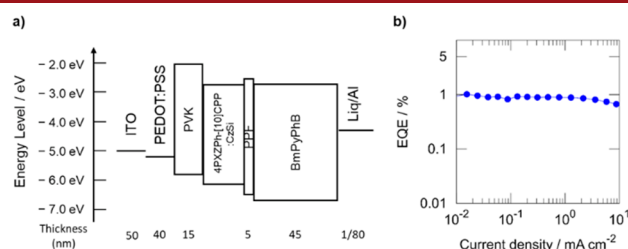


Figure 4. (a) Device stack of 4PXZPh-[10]CPP:CzSi based OLEDs. (b) EQE–current density characteristics.

(ITO) (50 nm)/poly(3,4-ethylenedioxythiophene)polystyrene sulfonate (PEDOT:PSS) (40 nm)/poly(9-vinylcarbazole) (PVK) (15 nm)/10 wt % 4PXZPh-[10]CPP:CzSi/dibenzo-[*b,d*]furan-2,8-diylbis(diphenylphosphine oxide) (PPF) (5 nm)/1,3-bis[3,5-di(pyridin-3-yl)phenyl]benzene (BmPyPhB) (45 nm)/lithium quinolin-8-olate (Liq) (1 nm)/Al (80 nm). PEDOT:PSS, PVK, and the emitting layers (EMLs) were deposited by spin-coating, and the other layers were thermally vacuum-deposited. In the device, PEDOT:PSS and PVK were used as a hole injection and transporting layers, respectively, BmPyPhB was used as an electron transporting and injection layer, and PPF was used as an exciton blocking layer. The fabricated OLED exhibits sky-blue emission with $\lambda_{\text{EL}} = 465$ nm, and the EQE_{max} of 1.0% (Figure 4b). The theoretical EQE_{max} (η_{ext}) is deduced from eq 1.

$$\eta_{\text{ext}} = \gamma \times \eta_r \times \Phi_{\text{PL}} \times \eta_{\text{out}} \quad (1)$$

Here, γ , η_r , and η_{out} are the charge carrier balance, emissive exciton production efficiency, and light out coupling efficiency, respectively. Assuming that 4PXZPh-[10]CPP is a conventional fluorescence material, and γ , η_r , and η_{out} are unity, 0.25, and 0.2, respectively, considering that Φ_{PL} is 0.29, the

experimental EQE_{MAX} is close to η_{ext} . Although the device performance is below satisfactory, this is the first report of an electroluminescent device employing a donor–acceptor CPP-based emitter material.

In summary, we designed a D–A CPP compound that was expected to show TADF. The DFT calculations revealed that this compound possesses a suitable HOMO/LUMO separation and the TDA-DFT calculation predicted a small ΔE_{ST} of 0.08 eV. **4PXZPh-[10]CPP** exhibited green emission in PhMe with $\lambda_{\text{PL}} = 508$ nm, $\Phi_{\text{PL}} = 34\%$, and a prompt lifetime of 11.0 ns. In the ambipolar host CzSi, **4PXZPh-[10]CPP** is moderately bright and showed sky-blue emission with $\lambda_{\text{PL}} = 475$ nm and $\Phi_{\text{PL}} = 29\%$ in the 15 wt % doped CzSi film. The solution-processed OLEDs based on **4PXZPh-[10]CPP** showed low efficiency due to a combination of low Φ_{PL} and inefficient RISC. The device with **4PXZPh-[10]CPP** in CzSi as the EML exhibited sky-blue emission, with λ_{EL} of 465 nm and an EQE_{max} of 1.0% at 1 mA cm^{-2} .

■ ASSOCIATED CONTENT

Data Availability Statement

The research data supporting this publication can be accessed at <https://doi.org/10.17630/6c910af5-0115-4e0f-8de8-faa484e406d1>.

Supporting Information

The Supporting Information is available free of charge at <https://pubs.acs.org/doi/10.1021/acs.orglett.3c00127>.

Experimental data, ^1H NMR, ^{13}C NMR, HRMS, HPLC report, and elemental analysis for all new compounds. Computation details, Natural transition orbitals analysis, UV–vis and fluorescence spectra, steady-state PL spectra, emission spectra, chromatogram, photophysical measurements, cyclic voltammetry, CV plot, and device fabrication details (PDF)

Atomic coordinates (TXT)

■ AUTHOR INFORMATION

Corresponding Authors

Shigeru Yamago – Institute for Chemical Research, Kyoto University, Uji 611-0011, Japan; orcid.org/0000-0002-4112-7249; Email: yamago@sci.kyoto-u.ac.jp

Hironori Kaji – Institute for Chemical Research, Kyoto University, Uji 611-0011, Japan; orcid.org/0000-0002-5111-3852; Email: kaji@sci.kyoto-u.ac.jp

Eli Zysman-Colman – Organic Semiconductor Centre, EaStCHEM School of Chemistry, University of St. Andrews, St. Andrews, Fife KY16 9ST, United Kingdom; orcid.org/0000-0001-7183-6022; Email: eli.zysman-colman@st-andrews.ac.uk

Authors

Dongyang Chen – Organic Semiconductor Centre, EaStCHEM School of Chemistry, University of St. Andrews, St. Andrews, Fife KY16 9ST, United Kingdom

Yoshimasa Wada – Institute for Chemical Research, Kyoto University, Uji 611-0011, Japan; orcid.org/0000-0001-6139-8794

Yu Kusakabe – Institute for Chemical Research, Kyoto University, Uji 611-0011, Japan

Liansheng Sun – Institute for Chemical Research, Kyoto University, Uji 611-0011, Japan

Eiichi Kayahara – Institute for Chemical Research, Kyoto University, Uji 611-0011, Japan; orcid.org/0000-0003-1663-5273

Katsuaki Suzuki – Institute for Chemical Research, Kyoto University, Uji 611-0011, Japan

Hiroyuki Tanaka – Institute for Chemical Research, Kyoto University, Uji 611-0011, Japan

Complete contact information is available at: <https://pubs.acs.org/doi/10.1021/acs.orglett.3c00127>

Notes

The authors declare no competing financial interest.

This manuscript has been deposited to preprint repository ChemRxiv.¹

■ ACKNOWLEDGMENTS

We thank JSPS Core-to-Core Program and International Joint Usage/Research Program of Institute for Chemical Research, Kyoto University (grant #2020-37 and 2021-37) for financial support. The St Andrews team would also like to thank EPSRC (EP/P010482/1) for financial support. D.C. thanks the China Scholarship Council (No. 201603780001). The Kyoto team would like to thank JSPS KAKENHI Grant Numbers JP20H05840 (Grant-in-Aid for Transformative Research Areas, “Dynamic Exciton”).

■ REFERENCES

- (1) Chen, D.; Wada, Y.; Kusakabe, Y.; Kayahara, E-Ichi.; Sun, L.; Suzuki, K.; Tanaka, H.; Yamago, S.; Kaji, H.; Zysman-Colman, E. A Donor-Acceptor 10-Cycloparaphenylene and Its Use as an Emitter in an Organic Light-Emitting Diodes. *ChemRxiv* **2022**, DOI: [10.26434/chemrxiv-2022-41pf6](https://doi.org/10.26434/chemrxiv-2022-41pf6).
- (2) Omachi, H.; Segawa, Y.; Itami, K. Synthesis of Cycloparaphenylenes and Related Carbon Nanorings: A Step toward the Controlled Synthesis of Carbon Nanotubes. *Acc. Chem. Res.* **2012**, *45* (8), 1378–1389.
- (3) Golder, M. R.; Jasti, R. Syntheses of the Smallest Carbon Nanohoops and the Emergence of Unique Physical Phenomena. *Acc. Chem. Res.* **2015**, *48* (3), 557–566.
- (4) Yamago, S.; Kayahara, E.; Iwamoto, T. Organoplatinum-Mediated Synthesis of Cyclic π -Conjugated Molecules: Towards a New Era of Three-Dimensional Aromatic Compounds. *Chem. Rec.* **2014**, *14* (1), 84–100.
- (5) Darzi, E. R.; Hirst, E. S.; Weber, C. D.; Zakharov, L. N.; Lonergan, M. C.; Jasti, R. Synthesis, Properties, and Design Principles of Donor-Acceptor Nanohoops. *ACS Cent. Sci.* **2015**, *1* (6), 335–342.
- (6) Tang, Y.; Li, J.; Du, P.; Zhang, H.; Zheng, C.; Lin, H.; Du, X.; Tao, S. Fullerene’s Ring: A New Strategy to Improve the Performance of Fullerene Organic Solar Cells. *Org. Electron.* **2020**, *83*, 105747.
- (7) Aydin, G.; Koçak, O.; Güleriyüz, C.; Yavuz, I. Structural Order and Charge Transfer in Highly Strained Carbon Nanobelts. *New J. Chem.* **2020**, *44* (36), 15769–15775.
- (8) Jasti, R.; Bhattacharjee, J.; Neaton, J. B.; Bertozzi, C. R. Carbon Nanohoop Structures. *J. Am. Chem. Soc.* **2008**, *130*, 17646–17647.
- (9) Takaba, H.; Omachi, H.; Yamamoto, Y.; Bouffard, J.; Itami, K. Selective Synthesis of [12]Cycloparaphenylene. *Angew. Chemie - Int. Ed.* **2009**, *48* (33), 6112–6116.
- (10) Yamago, S.; Watanabe, Y.; Iwamoto, T. Synthesis of [8]Cycloparaphenylene from a Square-Shaped Tetranuclear Platinum Complex. *Angew. Chemie - Int. Ed.* **2010**, *49* (4), 757–759.
- (11) Kayahara, E.; Sun, L.; Onishi, H.; Suzuki, K.; Fukushima, T.; Sawada, A.; Kaji, H.; Yamago, S. Gram-Scale Syntheses and Conductivities of [10]Cycloparaphenylene and Its Tetraalkoxy Derivatives. *J. Am. Chem. Soc.* **2017**, *139* (51), 18480–18483.

- (12) Kayahara, E.; Patel, V. K.; Xia, J.; Jasti, R.; Yamago, S. Selective and Gram-Scale Synthesis of [6]Cycloparaphenylene. *Synlett* **2015**, 26 (11), 1615–1619.
- (13) Iwamoto, T.; Watanabe, Y.; Sakamoto, Y.; Suzuki, T.; Yamago, S. Selective and Random Syntheses of [n]Cycloparaphenylenes (n = 8–13) and Size Dependence of Their Electronic Properties. *J. Am. Chem. Soc.* **2011**, 133 (21), 8354–8361.
- (14) Segawa, Y.; Fukazawa, A.; Matsuura, S.; Omachi, H.; Yamaguchi, S.; Irle, S.; Itami, K. Combined Experimental and Theoretical Studies on the Photophysical Properties of Cycloparaphenylenes. *Org. Biomol. Chem.* **2012**, 10 (30), 5979–5984.
- (15) Kawanishi, T.; Ishida, K.; Kayahara, E.; Yamago, S. Selective and Gram-Scale Synthesis of [8]Cycloparaphenylene. *J. Org. Chem.* **2020**, 85 (4), 2082–2091.
- (16) Kayahara, E.; Kouyama, T.; Kato, T.; Yamago, S. Synthesis and Characterization of [n]CPP (n = 5, 6, 8, 10, and 12) Radical Cation and Dications: Size-Dependent Absorption, Spin, and Charge Delocalization. *J. Am. Chem. Soc.* **2016**, 138 (1), 338–344.
- (17) Fujitsuka, M.; Cho, D. W.; Iwamoto, T.; Yamago, S.; Majima, T. Size-Dependent Fluorescence Properties of [n]-Cycloparaphenylenes (n = 8–13), Hoop-Shaped π -Conjugated Molecules. *Phys. Chem. Chem. Phys.* **2012**, 14 (42), 14585–14588.
- (18) Lovell, T. C.; Fosnacht, K. G.; Colwell, C. E.; Jasti, R. Effect of Curvature and Placement of Donor and Acceptor Units in Cycloparaphenylenes: A Computational Study. *Chem. Sci.* **2020**, 11 (44), 12029–12035.
- (19) Lovell, T. C.; Garrison, Z. R.; Jasti, R. Synthesis, Characterization, and Computational Investigation of Bright Orange-Emitting Benzothiadiazole [10]Cycloparaphenylene. *Angew. Chemie - Int. Ed.* **2020**, 59 (34), 14363–14367.
- (20) Graham, C.; Moral, M.; Muccioli, L.; Olivier, Y.; Pérez-Jiménez, Á. J.; Sancho-García, J. C. N-Doped Cycloparaphenylenes: Tuning Electronic Properties for Applications in Thermally Activated Delayed Fluorescence. *Int. J. Quantum Chem.* **2018**, 118 (12), e25562.
- (21) Hong, G.; Gan, X.; Leonhardt, C.; Zhang, Z.; Seibert, J.; Busch, J. M.; Bräse, S. A Brief History of OLEDs—Emitter Development and Industry Milestones. *Adv. Mater.* **2021**, 33 (9), 2005630.
- (22) Uoyama, H.; Goushi, K.; Shizu, K.; Nomura, H.; Adachi, C. Highly Efficient Organic Light-Emitting Diodes from Delayed Fluorescence. *Nature* **2012**, 492 (7428), 234–238.
- (23) Etherington, M. K.; Gibson, J.; Higginbotham, H. F.; Penfold, T. J.; Monkman, A. P. Revealing the Spin-Vibronic Coupling Mechanism of Thermally Activated Delayed Fluorescence. *Nat. Commun.* **2016**, 7, 13680.
- (24) Penfold, T. J.; Gindensperger, E.; Daniel, C.; Marian, C. M. Spin-Vibronic Mechanism for Intersystem Crossing. *Chem. Rev.* **2018**, 118, 6975–7025.
- (25) Dos Santos, P. L.; Chen, D.; Rajamalli, P.; Matulaitis, T.; Cordes, D. B.; Slawin, A. M. Z.; Jacquemin, D.; Zysman-Colman, E.; Samuel, I. D. W. Use of Pyrimidine and Pyrazine Bridges as a Design Strategy to Improve the Performance of Thermally Activated Delayed Fluorescence Organic Light Emitting Diodes. *ACS Appl. Mater. Interfaces* **2019**, 11 (48), 45171–45179.
- (26) Rajamalli, P.; Chen, D.; Li, W.; Samuel, I. D. W.; Cordes, D. B.; Slawin, A. M. Z.; Zysman-Colman, E. Enhanced Thermally Activated Delayed Fluorescence through Bridge Modification in Sulfone-Based Emitters Employed in Deep Blue Organic Light-Emitting Diodes. *J. Mater. Chem. C* **2019**, 7 (22), 6664–6671.
- (27) Kaji, H.; Suzuki, H.; Fukushima, T.; Shizu, K.; Suzuki, K.; Kubo, S.; Komino, T.; Oiwa, H.; Suzuki, F.; Wakamiya, A.; Murata, Y.; Adachi, C. Purely Organic Electroluminescent Material Realizing 100% Conversion from Electricity to Light. *Nat. Commun.* **2015**, 6, 8476.
- (28) Qiu, Z. L.; Tang, C.; Wang, X. R.; Ju, Y. Y.; Chu, K. S.; Deng, Z. Y.; Hou, H.; Liu, Y. M.; Tan, Y. Z. Tetra-Benzothiadiazole-Based [12]Cycloparaphenylene with Bright Emission and Its Supramolecular Assembly. *Angew. Chemie - Int. Ed.* **2020**, 59 (47), 20868–20872.
- (29) Kayahara, E.; Nakano, M.; Sun, L.; Ishida, K.; Yamago, S. Syntheses of Tetrasubstituted [10]Cycloparaphenylenes by a Pd-Catalyzed Coupling Reaction. Remarkable Effect of Strain on the Oxidative Addition and Reductive Elimination. *Chem. - An Asian J.* **2020**, 15 (16), 2451–2455.
- (30) Adamo, C.; Barone, V. Toward Reliable Density Functional Methods without Adjustable Parameters: The PBE0Model. *J. Chem. Phys.* **1999**, 110 (13), 6158–6170.
- (31) Moral, M.; Muccioli, L.; Son, W. J.; Olivier, Y.; Sancho-García, J. C. Theoretical Rationalization of the Singlet-Triplet Gap in OLEDs Materials: Impact of Charge-Transfer Character. *J. Chem. Theory Comput.* **2015**, 11 (1), 168–177.
- (32) Goushi, K.; Yoshida, K.; Sato, K.; Adachi, C. Organic Light-Emitting Diodes Employing Efficient Reverse Intersystem Crossing for Triplet-to-Singlet State Conversion. *Nat. Photonics* **2012**, 6 (4), 253–258.
- (33) Rajamalli, P.; Senthilkumar, N.; Gandeepan, P.; Huang, P.-Y.; Huang, M.-J.; Ren-Wu, C.-Z.; Yang, C.-Y.; Chiu, M.-J.; Chu, L.-K.; Lin, H.-W.; Cheng, C.-H. A New Molecular Design Based on Thermally Activated Delayed Fluorescence for Highly Efficient Organic Light Emitting Diodes. *J. Am. Chem. Soc.* **2016**, 138 (2), 628–634.
- (34) Wei, X.; Chen, Y.; Duan, R.; Liu, J.; Wang, R.; Liu, Y.; Li, Z.; Yi, Y.; Yamada-Takamura, Y.; Wang, P.; Wang, Y. Triplet Decay-Induced Negative Temperature Dependence of the Transient Photoluminescence Decay of Thermally Activated Delayed Fluorescence Emitter. *J. Mater. Chem. C* **2017**, 5, 12077–12084.